HOW DIRECT MARKETING OF A WIND FARM AFFECTS OPTIMAL DESIGN AND OPERATION OF VANADIUM REDOX FLOW BATTERIES

Sebastian König, Konstantinos Iliopoulos, Michael R. Suriyah and Thomas Leibfried
Karlsruhe Institute of Technology,
Institute of Electric Power Systems and High-Voltage Technology,
Karlsruhe, Germany
E-Mail: sebastian.koenig@kit.edu

1 Introduction

1.1 General introduction

Storing electric energy supports the transition of an electric power system from fossil fuels towards renewable energy sources (RES) in many ways. Possible applications range from peak shaving of photovoltaic power plants over grid services to seasonal balancing of fluctuating RES [1]. The intended use case for the storage system has an influence on choice of technology as well as on system design and operation. Model-based battery system optimization can be improved by embedding simulation of the intended application. Considering the application delivers a more significant optimization criterion, such as actual efficiency or total energy losses, than the isolated simulation of the battery.

1.2 Introduction of the all-vanadium redox flow battery

Among battery energy storage technologies flow batteries have several advantages, if the storage is supposed to deliver rated power for more than four hours. Flow batteries store energy in liquid electrolyte, which is placed in separate tanks and is supplied to the stacks via closed-loop circuits. In all-vanadium redox flow batteries (VRFB) the electrolyte consists of vanadium ions, dissolved in diluted sulfuric acid.

Energy and power rating of a flow battery is completely decoupled. Number and dimensions of the battery stacks determine the power. Number and volume of the tanks determine the capacity. Therefore, large storage capacities only require large tanks and a large amount of electrolyte, but do not affect the battery's active parts. This will be very cost effective as soon as electrolyte production for VRFBs turns from niche to mass market. Furthermore, VRFB technology has a very low toxicology and is intrinsic explosion and fire save [2].

In a large scale VRFB, several stacks are electrically connected in series to a string, to boost battery voltage and to facilitate grid connection. Several strings are connected to one pair of tanks. The two tanks and the connected stacks are called battery module. According to the required battery power, the number of deployed modules is determined. The tank volumes of the module are determined by the energy storage demand. Additional design parameters such as pipe diameters and cell design can be optimized according to power value's frequency distribution of the application. In this work, the battery is used to support direct marketing of a wind farm.

1.3 Introduction of direct marketing

Starting from 1st of August 2014, direct marketing of RES is mandatory for new plants exceeding 500 kW, according to the revised German Renewable Energy Sources Act (EEG) 2014 [3]. This especially affects wind farms, as every wind turbine easily exceeds given limitation for direct marketing. However, fluctuating nature of the wind does not allow single wind power plants or wind farms to participate in power derivatives market. Day-ahead and intraday market are better suited, because very precise weather forecasts are available for the bidding time span. Here, we only consider day-ahead marketing, as intraday wind forecast was not available. Battery storage systems can be used to ensure that energy, sold in day-ahead market, is delivered in spite of forecast errors and thus prevent or at least reduce purchase of expensive balancing energy.

2 Methodology

2.1 General methodology

The presented work consists of two parts. First, a multi-physical flow battery model is used to simulate efficiency of a battery module. Module design is varied to achieve different efficiencies under partial and full load conditions. Battery capacity is varied as well to determine a reasonable storage size. Using the day ahead marketing simulation of a wind farm, we decide which design delivers best results for the given purpose.

Battery efficiency is always depending on system power and state of charge (SOC). For simplification, SOC dependance is neglected here. Power dependent efficiency has to be averaged to obtain a distinct quality criterion for optimization. It is reasonable to weight efficiency at different power levels according to the power magnitude of each level. However if not all power levels appear equally frequent, additional weighting factors should be introduced, as shown in (1). Therein, N_{Level} is number of the simulated power levels, w is the additional weighting factor, P is power and η_{i} is efficiency at power level i.

$$\eta_{\mathrm{Sys}} = \frac{\sum_{i=1}^{N_{\mathrm{Level}}} \left(w_{\mathrm{i}} \cdot P_{\mathrm{i}} \cdot \eta_{\mathrm{i}} \right)}{\sum_{i=1}^{N_{\mathrm{Level}}} \left(w_{\mathrm{i}} \cdot P_{\mathrm{i}} \right)} \tag{1}$$

Weighting factors could be derived by first simulating battery supported day-ahead marketing of the wind farm without considering battery efficiency. Efficiency is not available yet, as battery design is still unknown. This would however neglect the fact, that battery efficiency itself influences power value's frequency distribution. Therefore, we first simulate a variety of designs, whose efficiencies are afterwards implemented into day-ahead marketing simulation. This simulation then delivers the desired criterion, which allows for a decision between the simulated designs. Alternatively, battery and application simulation could also be conducted iteratively.

The implemented flow battery is assumed to consist of 50 modules which results in a rated system discharging power of 2 MW and a rated system charging power of 3 MW. Power boundaries are non-symmetrical because power is limited due to current constraints and string voltage is higher during charging than during discharging of the battery. The power, required to support the wind farm, is dispatched to the modules in an optimized way, see Section 2.4. Direct marketing is simulated for the year 2013.

2.2 Flow battery modeling

The model used in this study is presented in detail in Ref. [4], where all additional system parameters are published as well. Here we introduce the most important equations and parameters, see Table 1.

Tab. 1: Important battery system parameters

Total vanadium concentration	1.6 mol/l
Number of cells per stack	30
Formal cell potential	1.4 V
Stack series resistance	20 mΩ
Stack hydraulic resistance	$68.7\,\frac{\mathrm{kPa\cdot s}}{\mathrm{l}}$

2.2.1 Cell voltage and SOC

Cell voltage is derived from cell SOC using the simplified Nernst equation:

$$E(t) = E'^{0} + 2\frac{GT}{F}\ln\left(\frac{SOC(t)}{1-SOC(t)}\right). \tag{2}$$

Therein $E(t)$ is cell voltage, G is the universal gas constant, T is temperature and F is the Faraday constant. E'^{0} is the formal cell potential which also considers the contribution of the hydrogen-ions.

SOC is derived as follows, using c_2 for concentration of V^{2+}-ions, c_3 for concentration of V^{3+}-ions and c_V for total vanadium concentration:

$$SOC(t) = \frac{c_2(t)}{c_2(t)+c_3(t)} = \frac{c_2(t)}{c_V} = 1 - \frac{c_3(t)}{c_V}. \tag{3}$$

Cell SOC is derived from cell concentration of V^{3+}-ions:

$$c_{3,\mathrm{C}}(t_1) = c_{3,\mathrm{C}}(t_0) + \frac{1}{V_\mathrm{C}} \cdot \left(\left(c_{3,\mathrm{T}}(t_0) - c_{3,\mathrm{C}}(t_0)\right) \cdot Q_\mathrm{C}(t_0) - \frac{I(t_0)}{F} \right) \cdot (t_1 - t_0). \tag{4}$$

Therein $c_{3,\mathrm{C}}$ is cell concentration of V_3-ions, V_C is cell volume, $c_{3,\mathrm{T}}$ is tank concentration of V_3-ions, I is cell's load current and Q_C is cell's volumetric electrolyte flow rate. The current and the previous simulation time step is denoted t_1 and t_0 respectively.

Referred to vanadium ion concentration, SOC is allowed to vary between 20 % and 80 %. In the following, all given battery capacities are obtained between these two limits, from now on referred to as 0 % and 100 % relative SOC.

2.2.2 Considered loss mechanisms

- Ohmic losses are considered using a constant resistor in the equivalent electric circuit.
- Concentration over-potential is modeled as presented in Refs. [5, 6].
- Shunt current losses are considered using the equivalent electric circuit of the shunt current network, equipped with SOC-dependent resistors [4].
- Pump losses are computed by simulating both hydraulic circuits of the battery. Flow rate dependent pump efficiency is considered as well.
- Losses of energy conversion system (ECS) are considered using a look-up table with values derived from manufacturer data sheets.

2.3 Module designs

The module considered in this study is shown in Fig. 1 with two 8,000 l tanks. Tank volume corresponds to a regular capacity of 250 kWh. Pipes which are directly connected to one of the tanks are denoted main pipes. Pipes connecting stacks and main pipes are called branch pipes. Within the anolyte circuit, main pipe length is 22.15 m, compared to 16.36 m in the catholyte circuit. Between each stack there is a main pipe with 1 m length. Branch pipe length from main pipe to stack is 0.2 m in each circuit. From stack back to main pipe, branch pipe length is 0.95 m.

Basic stack design is taken from Refs. [7, 8]. In this work, the balance between shunt current losses and required power for pumping the electrolyte is used to obtain different efficiencies under partial and full load conditions. Shunt currents occur because all cells of a string are electrically connected in series, but hydraulically connected in parallel. They all use a common manifold in each stack and common outer circuitry. As the electrolyte is a bad insulator, potential differences between cells and stacks lead to electric currents occurring in the electrolyte. If more cells are electrically connected in series using a common hydraulic circuit, shunt currents increase significantly [4, 8]. Here, three stacks are connected in series and two of these strings are connected in parallel to form the module with a rated charging power of 60 kW and a rated discharging power of 40 kW.

Effect of shunt currents can be reduced, if the active cell area is connected to common inlet and outlet manifold via two channels in the shape of meanders, see Fig. 2. This extends shunt current path artificially and therefore increases effective electric resistance of the electrolyte path. Channels can be prolonged by adding more meander turns. This of course also increases stack hydraulic resistance. The same two effects occur, if narrower pipes are used in the hydraulic circuit.

While shunt current losses occur all the time, even if the battery is idle, pump losses strongly increase with battery load. Therefore, longer channels and narrower pipes increase the efficiency especially under light load conditions. This is because the small required load current does only require a small volumetric electrolyte flow rate, which requires fewer pumping power. Thus the design reduces shunt currents, but does not cause much additional pump power at light loads. However, if the battery has to deliver rated power, additional pressure drop due to longer channels and narrower pipes cause additional losses, which cannot be compensated by the prevented shunt current losses. It is obvious, that such a design is better suited for applications where long periods of partial loads occur. If rated power is required very often, a shorter channel and wider pipes will deliver a better performance. Five different designs, starting with very long channels and narrow pipes going to shorter channels and wider pipes are given in Table 2.

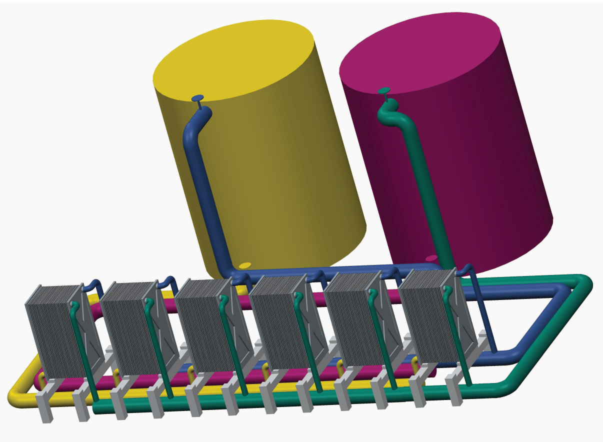

Fig. 1: 250 kWh battery module

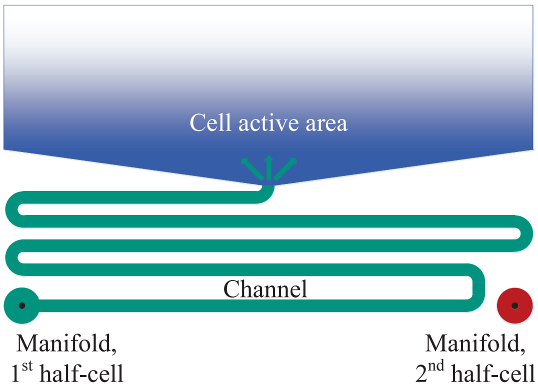

Fig. 2: Channel with five turns

2.4 Optimized operation - Module dispatch

The large number of available modules in a large scale battery offers a big optimization potential. The green, continuous line in Fig. 4 exemplarily shows charging efficiency curve of a flow battery module with a rated charging power of 60 kW. At low power, system efficiency suffers from low

ECS efficiency as well as from shunt currents. At high power, ohmic losses and pumping energy account for the biggest share of the losses. At approximately 50 % of its rated power, the module reaches its efficiency peak. Up to this power it is optimal to use only one module.

If more power is required two questions have to be answered. When should the number of active modules be increased and how should power be distributed between all active modules? The optimal answers to these two questions are very hard to find for a system with 50 modules.

We propose a solution, which answers the second question first: Power is always equally distributed between all active modules. The number of modules which should be activated is then very easy to find. If more than one module is active, efficiency curve just has to be scaled along the x-axis using the number of active modules as scaling factor. For two active modules, the efficiency curve is the same as for one module, but it is scaled from zero to 120 kW instead from zero to 60 kW. Three active modules would range from zero to 180 kW and so on, as shown in Fig. 4. Thereby every intersection of two neighboring curves indicates a change in the number of active modules.

Although this approach does not deliver the optimal power dispatch, it achieves an efficiency very close to the optimum. For a two module system, the optimal load dispatch is fairly easy to compute. Compared to the proposed solution, the second module is activated at a power level that is 40 W smaller. This results in a system efficiency that is increased by 0.01 %, which does not sanctify the additional effort for the computation. If more modules are active, the difference between our approach and the optimal dispatch will be even smaller, as the impact of every single module on system efficiency becomes smaller, the more modules are active.

2.5 Direct marketing of the wind farm

The examined wind farm with a peak power of 12 MW is located near the city of Cottbus in North-East Germany. Power forecast of the wind farm is completely marketed via the day-ahead market, complying with the market rules, see Ref. [9]. Day-ahead power forecast was delivered by Enercast GmbH, a spin-off company of Fraunhofer IWES, which is specialized on forecasting renewable energy in-feed. Root mean square error (RMSE) of the forecast for 2013 was 8.6 %. Forecast and actual power in-feed for March 2013 is exemplarily shown in Fig. 3. Forecast time resolution is 15 min. The day-ahead market only allows energy blocks of 100 kW power and 1 h time spacing. Therefore, the four forecast values of every hour are averaged and rounded to multiples of 100 kWh.

Flow battery's task is to even out the forecast error. Limitations are battery power and battery capacity. If the SOC limit is violated, the battery is switched off until power flow direction can be reversed. If the battery is charged, charging power is multiplied with charging efficiency and then integrated to obtain the SOC. If the battery is discharged, required discharging power is divided by discharging efficiency to obtain the power which is actually drawn out of the tanks, which is

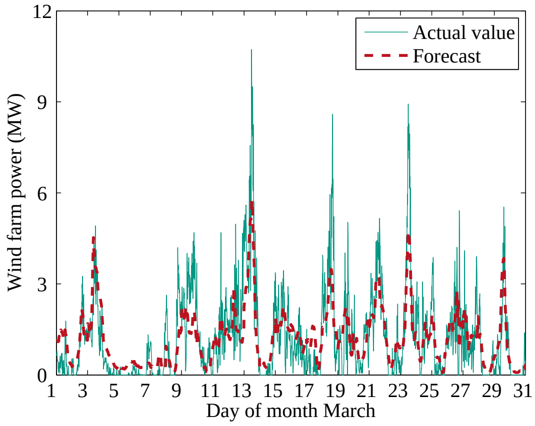

Fig. 3: Forecast and actual value of power in-feed for March 2013

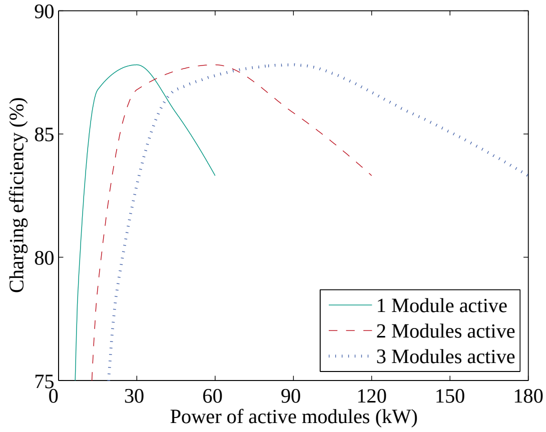

Fig. 4: Charging efficiency, up to three modules active

then integrated as well.

3 Results

3.1 Battery simulations and optimized module dispatch

System charging and discharging efficiencies are shown in Fig. 5. Design efficiencies vary strongly under partial and full load conditions. Negative power corresponds with battery discharging. Power weighted average efficiency does only vary slightly, see Table 2. This weighting assumes, that all power levels are used equally frequent. If no information about the power value's frequency distribution for the application is available, it could also serve as optimization criterion.

Especially under partial load conditions, efficiency gain due to optimized module dispatch is significant, see Fig. 6 (area between green, continuous line and blue, dotted line).

Tab. 2: Considered battery designs

	Design 1	Design 2	Design 3	Design 4	Design 5
Main pipe diameter	80 mm	100 mm	120 mm	140 mm	160 mm
Branch pipe diameter	20 mm	25 mm	30 mm	35 mm	40 mm
Channel number of turns	8	7	6	5	4
		Results			
Average efficiency	67.7 %	68.2 %	68.1 %	67.8 %	67.2 %
Bat. losses (30 MWh Capacity)	636 MWh	637 MWh	647 MWh	665 MWh	691 MWh

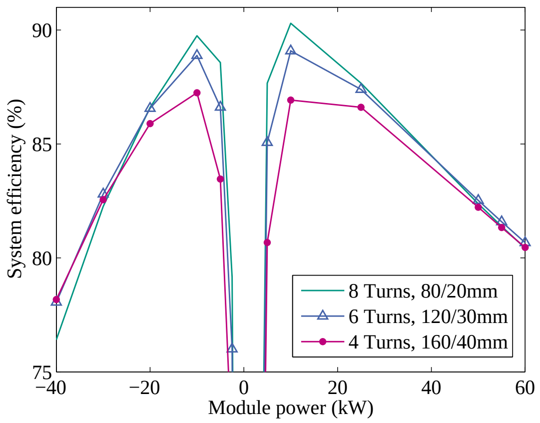

Fig. 5: Simulated system efficiencies, Design 1,3 and 5

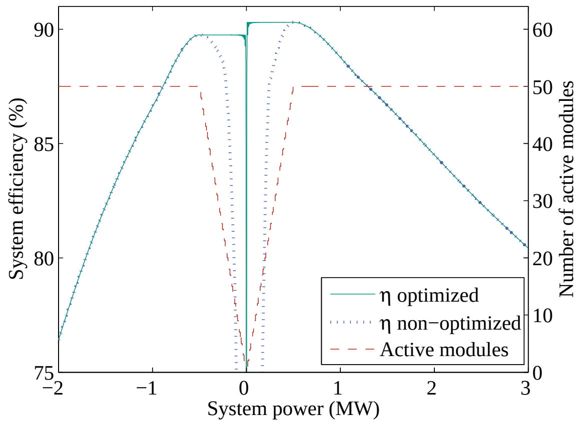

Fig. 6: Optimized module dispatch, Design 1

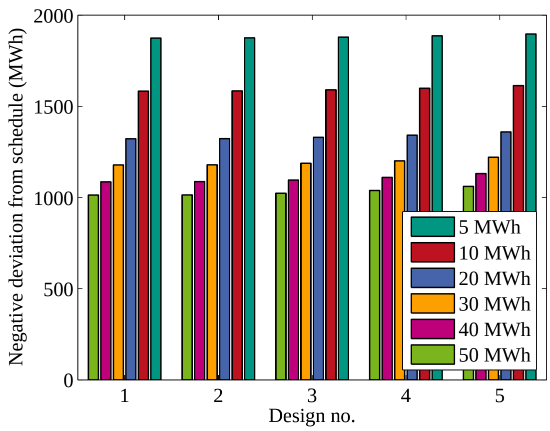

Fig. 7: Negative deviations from schedule in 2013

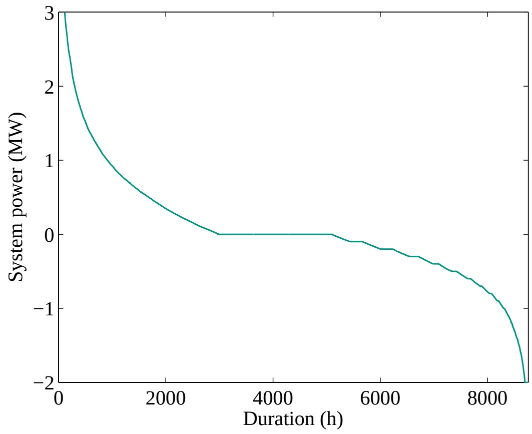

Fig. 8: Battery power duration curve for 30 MWh capacity in 2013

3.2 Direct marketing of the wind farm

As the complete forecasted energy is placed on day-ahead market, its total value does not depend on the deployed battery design. In total 13,309 MWh can be sold. If no battery support is available, 3,020 MWh are delivered short of the schedule, 3,334 MWh exceeding the schedule.

With the battery negative and positive deviation from schedule can be reduced with every design. Here we focus on negative deviations, as positive deviations could easily be prevented by reducing the wind farm power, if the battery is already fully charged.

For all designs, a significant deviation from the day-ahead schedule remains, see in Fig. 7. If a 50 MWh capacity is deployed, negative deviations from schedule can be reduced to 1,014 MWh. However for capacities larger than 30 MWh, reduction of negative schedule deviations becomes rather small. For all capacities, Design 1 causes the smallest losses and thus is able to support day-ahead marketing best.

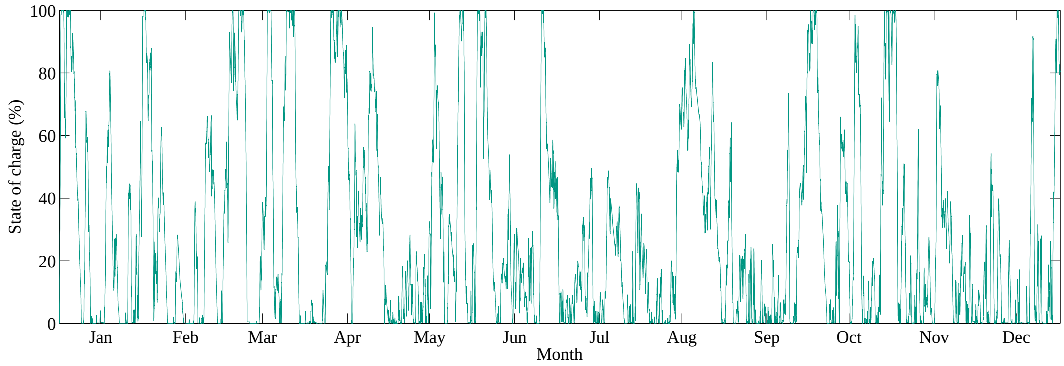

Fig. 9: SOC of the 30 MWh battery in 2013

Fig. 8 explains why for this use case obviously efficiency under partial load conditions is more important. The graph shows charging and discharging power, sorted after time period of occurrence. At a vast majority of time, the battery only operates under very light load. More than 5,400 h in 2013, the power magnitude was below 500 kW. The step at -2 MW and 3 MW shows, that the battery cannot fulfill power demand for balancing the forecast error at all the times. However a battery with infinite capacity would reduce negative deviations from schedule to only 61 MWh, with the same power constraints. The large remaining deviation is therefore to explain by capacity constraints, which can also be seen in Fig. 9. SOC reaches its upper or lower limit rather often.

4 Discussion and conclusion

The implementation of simulated battery efficiencies into day-ahead marketing simulation identifies Design 1 as optimal design while power weighted average efficiency chooses Design 2. However, difference in losses between these two designs is rather small. Nevertheless, compared to Design 4, which also shows a higher average efficiency as Design 1, losses are reduced by 29 MWh. It is therefore reasonable, to combine battery and use case simulation, in order to derive a significant quality criterion for model-based optimization.

Power duration curve however shows, that more efforts should be done, to boost partial load efficiency, accepting a certain efficiency drop at rated power. The proposed optimized module dispatch is an important step in boosting partial load efficiency of the overall system. It is important to mention, that demonstrated values are only realistic, if all idle modules are not causing any losses. This means, that the energy which is stored in the module's stacks has to be withdrawn by the ECS, if the module is deactivated.

By supporting the 12 MW-wind farm with a large VRFB of up to 50 MWh of capacity, power deviation during day-ahead marketing has been drastically reduced. Nevertheless there still remains a significant deviation, which is first of all due to the SOC constraints. Of course, larger capacities could further reduce the deviations, but are prevented out of economic reasons.

Whether the battery is profitable or not strongly depends on costs due to balancing energy. The energy placed in day-ahead market is not increased by the battery. Therefore only prevented balancing energy costs are earned by the battery system. However beside battery storage, there are other ways of dealing with the schedule deviations. First of all, intraday market could be used. Furthermore pooling of plants or contracting better controllable power plants for backup are additional possibilities, which of course cause certain costs as well. Nevertheless, among all battery technologies, redox flow batteries are best suited for this use case, as rather large storage capacities are required to effectively support direct marketing. Other applications such as delivering grid services could be integrated into the considered use case to enhance economics.

References

[1] Agora-Energiewende. Study: Stromspeicher für die Energiewende. `http://www.agora-energiewende.de/fileadmin/downloads/publikationen/Studien/Speicher_in_der_Energiewende/Agora_Speicherstudie_Web.pdf`, 2014.

[2] Piergiorgio Alotto, Massimo Guarnieri, and Federico Moro. Redox flow batteries for the storage of renewable energy: A review. *Renew. and Sustainable Energy Reviews*, 29(0):325 – 335, 2014.

[3] Federal Ministry of Justice and Consumer Protection. Renewable Energy Sources Act - EEG 2014. `http://www.gesetze-im-internet.de/bundesrecht/eeg_2014/gesamt.pdf`, 07/21/2014.

[4] S. König, M. Suriyah, and T. Leibfried. Model based examination on influence of stack series connection and pipe diameter on efficiency of vanadium redox flow batteries under consideration of shunt currents. *J. Power Sources*, 2015.

[5] Ao Tang, Jie Bao, and Maria Skyllas-Kazacos. Studies on pressure losses and flow rate optimization in vanadium redox flow battery. *J. Power Sources*, 248(0):154 – 162, 2014.

[6] S. König, M. Suriyah, and T. Leibfried. Volumetric electrolyte flow rate control in vanadium redox flow batteries using a variable flow factor. In *6th International Renewable Energy Congress (IREC)*, March 2015.

[7] S. König, M. Zimmerlin, T. Leibfried, F. Wandschneider, S. Röhm, and P. Fischer. Optimaler Aufbau von Batteriesystemen für Windkraftanlagen. In *International ETG-Congress, Berlin, Germany*, November 2013.

[8] F.T. Wandschneider, S. Röhm, P. Fischer, K. Pinkwart, J. Tübke, and H. Nirschl. A multi-stack simulation of shunt currents in vanadium redox flow batteries. *J. Power Sources*, 261(0):64 – 74, 2014.

[9] EPEX-SPOT. EPEX Spot Operational Rules. `http://www.epexspot.com/en/extras/download-center/documentation`, 11/12/2014.